Color and luminance spatial tuning estimated by noise masking in the absence of off-frequency looking

M. Angeles Losada and Kathy T. Mullen

McGill Vision Research, Department of Ophthalmology (H4.14), McGill University, 687 Pine Avenue West, Montreal, H3A 1A1 Canada

Received March 17, 1994; revised manuscript received September 8, 1994; accepted September 13, 1994

We assessed the contribution of off-frequency looking for pattern detection and obtained bandwidths for chromatic and luminance mechanisms in conditions free from this effect. We used a simultaneous spatial masking technique with Gaussian enveloped sinusoidal test stimuli (0.5 cycle/deg) and filtered one-dimensional static-noise masks whose spectral power was uniformly distributed per octave. Stimuli were modulated in the chromatic (isoluminant red–green) or the luminance (yellow–black) domain. Color and luminance detection thresholds were compared for low-pass, high-pass, and notch- (band-stopped) filtered noise. We obtained the following results: (1) at high-noise spectral densities, masking by notched noise is greater than the summed masking of the high- and low-pass noise, indicating the presence of off-frequency looking for both color and luminance detection. There is no evidence for off-frequency looking at lower power densities. (2) Using notch-filtered noise, which avoids the problem of off-frequency looking, we found that color processing is subserved by bandpass channels with bandwidths similar to those revealed for luminance processing. (3) Both color and luminance mechanisms appear to have bandwidths proportional to their center frequency (constant in octaves). (4) The lower and upper sides of the color and luminance tuning functions were estimated individually by use of high-pass and low-pass noise of a low power density and are revealed to be asymmetric, with the lower side declining more steeply than the upper side.

Key words: color vision, noise masking, spatial tuning, isoluminance.

1. INTRODUCTION

In luminance vision the existence of visual mechanisms acting in parallel, each selectively sensitive to a limited range of spatial frequencies, is widely accepted.[1,2] The spatial tuning of these mechanisms has been estimated by suprathreshold masking with sine-wave stimuli[3] and with visual noise.[4,5] Although the estimates of the bandwidths may vary, these studies are in overall agreement with other methods such as subthreshold summation[6] and spatial adaptation,[7] and they reveal luminance mechanisms with bandpass characteristics at detection threshold. Furthermore, recent psychophysical results based on sine-wave masking[8–12] and spatial adaptation[13] suggest that color vision, like luminance vision, encodes the scene into a range of spatial scales by bandpass filtering.

These previous masking studies have in general assumed that a single mechanism determines the detection threshold of the test stimulus, which simplifies the interpretation of the masking functions and allows the spatial tuning of the detection mechanisms to be derived directly from the masking data.[3–5,8,9] It has been proposed, however, that a more realistic model of test detection requires the supposition of multiple mechanisms, with peaks spanning the spatial-frequency range.[14–17] The assumption of multiple mechanisms complicates the determination of the spatial tuning of the detection mechanisms in a number of crucial ways. In particular, in the presence of high-contrast masking stimuli, the detection of the test may be subserved by mechanisms with a center frequency shifted away from the test frequency, thus optimizing the detection threshold. This effect was first found in auditory masking and termed off-frequency listening,[18] and the corresponding effect in vision has been termed off-frequency looking.[19] Evidence for test detection by multiple mechanisms has been found in spatial masking both with narrow-band noise[19–22] and with sine waves.[12,14–16] Off-frequency looking will narrow the estimates of the bandwidths of the detection mechanisms. Furthermore, since off-frequency looking may occur to different degrees depending on the stimulus conditions, accurate comparisons among different detection mechanisms are unreliable.

The aims of this paper are twofold. First, we assess the degree of off-frequency looking in the spatial processing of both luminance and color contrast, using a method of noise masking adapted from auditory techniques.[12,23,24] Second, we estimate the spatial tuning of both the chromatic and the luminance mechanisms without off-frequency looking and thus more closely indicate the tuning of the underlying color and luminance detection mechanisms. In Fig. 1 we illustrate the role of off-frequency looking and the methods that we use to remove its effects. The left-hand column illustrates the effects of noise for a single detection mechanism at threshold, and the right-hand column shows a multiple-(three) mechanism model of detection. The test spatial frequencies are marked with arrows. The area of overlap between the noise band and the mechanism tranfer function represents the amount of effective noise for that mechanism. The more sensitive mechanism (with the higher signal-to-noise ratio) is represented by the thick lines. Figures 1(a) and 1(b) show the effects of two different noise bands. For multiple mechanisms, the low-pass and the high-pass noise bands promote detection by mechanisms centered at frequencies adjacent to

0740-3232/95/020250-11$06.00

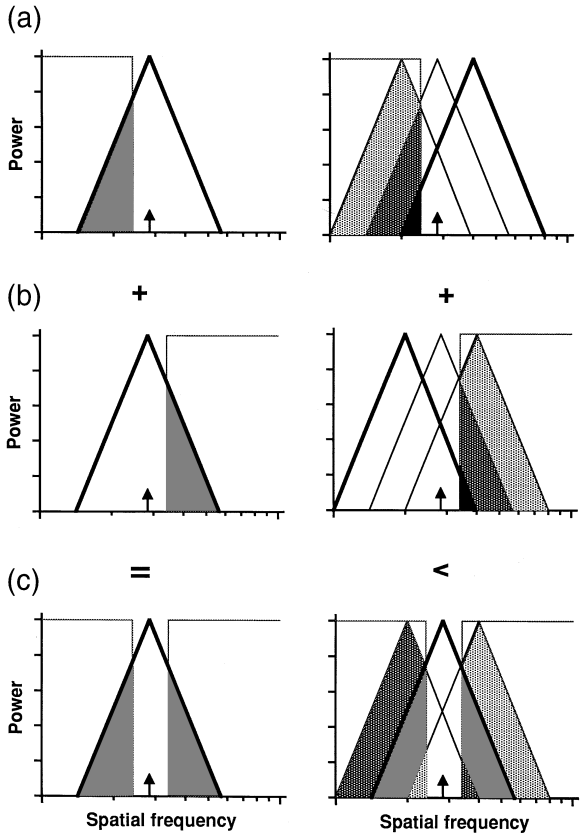

Fig. 1. Detection by single and multiple mechanisms. The effects of different noise bands are shown for detection by a single mechanism (left-hand column) and for multiple-mechanism detection (right-hand column). The noise bands are (a) low pass, (b) high pass, and (c) symmetric notched. Arrows mark test spatial frequencies. The transfer functions of the mechanisms are modeled by exponential functions. In the multiple-mechanism model, three mechanisms are shown, centered at the test frequency and ±0.5 octave from it. The area of overlap between the noise band and the mechanism transfer function, representing the amount of effective noise for that mechanism, is shaded with different grays for the different mechanisms. The mechanism with the higher signal-to-noise ratio is represented with a thick line.

the test frequency (off-frequency looking). For example, in Fig. 1(a), showing low-pass noise, the noise for the mechanism centered at the test frequency is greater than for the mechanism centered at the higher frequency, and thus it is the higher-frequency mechanism that has the better signal-to-noise ratio and determines test threshold. The equivalent effect occurs for high-pass noise [Fig. 1(b)]. Thus off-frequency looking will lower detection thresholds and narrow the estimates of the bandwidths.[15–17,20,22,25]

Off-frequency looking can be prevented by use of notch-filtered noise.[18,20,22–24] Symmetric notched noise is obtained by adding two noise bands with symmetric cutoffs above and below the test spatial frequency. Figure 1(c) illustrates how the presence of the second noise band prevents the use of multiple mechanisms for detecting the test. We use this method to estimate the passbands of the chromatic and luminance detection mechanisms. If only a single mechanism determines threshold, the masking obtained with notched noise will be equal to the summed masking for low- and high-pass noise (perfect summation), as illustrated in the left-hand panel of Fig. 1(c). In the presence of off-frequency looking, however, the masking obtained with notched noise will be greater than the summed masking obtained with low- and high-pass noise. This effect, known as excess of masking, reveals the intrusion of multiple mechanisms in test detection.[21] We compare the summed masking with the masking from a notch filter to estimate the presence of off-frequency looking in color and luminance noise masking.

A test frequency of 0.5 cycle/deg was chosen to reveal off-frequency looking in the color and luminance domains. This spatial frequency lies near a declining region of both the color and the luminance contrast-sensitivity functions,[26] thus optimizing the overall conditions for the intrusion of mechanisms centered at spatial frequencies on the more sensitive side with respect to the test frequency. We use noise whose power density is constant when spatial frequency is measured in octaves rather than in linear units. The choice of a power density that varies as $1/f$ is supported by previous psychophysical[3,5,7–9,12,13] and physiological[27–29] results that reveal the bandwidths of the spatial visual mechanisms to be proportional to their central spatial frequencies (i.e., constant in octaves). In addition, models based on self-similar transforms have been proposed as being more adequate for the processing of the information in natural scenes.[30] We provide further evidence that the bandwidths of spatial mechanisms are proportional to their central frequencies.

We find evidence of off-frequency looking at high-noise power densities with both high-pass and low-pass filtered noise for both color and luminance masking. At low power densities, however, low- and high-pass noise is free from the intrusion of multiple mechanisms in test detection. Bandwidth estimations with notched noise reveal bandpass mechanisms that are similar for both color and luminance contrast detection, having an average passband of 1.3 octaves. The disadvantage of the notched noise is the necessary assumption that the detection mechanism is symmetric about test frequency. Thus we have also estimated the lower- and upper-frequency sides of the tuning functions individually, using low- and high-pass noise at low power densities. These estimates reveal asymmetric tuning functions, with the lower side declining more steeply than the upper side.

2. METHODS

A. Stimuli and Apparatus

The stimulus generation and apparatus have been described in detail elsewhere.[26,31] Stimuli were produced by the display of two luminance-modulated gratings, each on a Joyce (DM2) display screen with white P4 phosphor; the gratings were viewed through narrow-band interference filters (Melles–Griot) with center wavelengths of 525 and 605 nm and full bandwidths at half-height of 21–22 nm. The two monochromatic gratings were combined spatially 180 deg out of phase by a beam splitter to produce a chromatic stimulus or in phase for a luminance stimulus of the same mean luminance and chromaticity. Longitudinal and transverse chromatic aberrations were corrected.[26] A bite bar was used to align the observer's head. Viewing was monocular with a natural pupil. Stimuli had a mean luminance of 22 cd m^{-2}

and were centrally fixated with use of a small fixation spot. All stimuli were generated with a VSG2/1 waveform generator (Cambridge Research Systems) with 14-bit analog output digital-to-analog converters. Linearized calibrations of the phosphors of the display monitors were made with a UDT optometer (Model 5370) fitted with a photometer head (#256). The goodness of the fits of the linearizing lookup tables to the light output of the monitors produced a contrast error for the displayed stimuli within 0.017 log unit.

Test stimuli were horizontal Gaussian enveloped red–green isoluminant gratings or isochromatic luminance gratings, usually of a spatial frequency of 0.5 cycle/deg. For some experiments, gratings of other spatial frequencies were used. Masking stimuli were static luminance or random chromatic modulations, displayed horizontally. Uncorrelated one-dimensional random-noise distributions were digitally generated and filtered in the Fourier domain with low-pass, high-pass, bandpass, and notched filters. Test and mask were Gaussian enveloped along the axis of modulation. The Gaussian width at $1/e$ of its maximum height was three test cycles. On the horizontal axis, test and mask were sharply truncated at a bar length of four cycles of the test stimulus. Thus the spatial extent of the stimuli was determined by the spatial frequency of the test grating, and the number of cycles in the masking stimulus varied inversely with the test spatial frequency.

Contrast of the two luminance component gratings was defined by

$$C = (I_{\max} - I_{\min})/(I_{\max} + I_{\min}), \tag{1}$$

where $I_{\max}$ and $I_{\min}$ are the peak and the trough luminance values of the monochromatic grating, respectively. For determining isoluminance, the mean luminances of the two component gratings were varied while their contrasts were held constant. The contrasts of both the isoluminant chromatic grating and the homochromatic luminance grating are defined as the contrast of the component gratings, C. Isoluminance of the two colors was measured with a minimum-motion method. Subjects varied the ratio of the red-to-green mean luminance in the stimulus with a method of adjustment to find the point at which the perceived drift rate of a sine-wave grating reached a minimum. This procedure was repeated at least 10 times and an average obtained. This is a convenient method of obtaining the isoluminant point, as there is a sharply defined minimum in perceived drift rate at isoluminance for these stimuli.[31–33]

B. Psychophysical Methods

Thresholds were measured with a standard two-alternative–forced-choice staircase procedure. The masking stimulus appeared in each of two time intervals and was accompanied by the test stimulus in one interval. The noise pattern was different in each interval, and a new pair was used for every trial. The stimulus was presented with a temporal Gaussian envelope with a spread at $1/e$ of 125 ms. The stimulus was stationary, and the phase of its presentation within the envelope was randomly varied between intervals. The subject indicated, by pressing a button, in which interval the test stimulus had appeared, and feedback was given after each trial. The staircase procedure was terminated after a minimum of eight reversals in the contrast presented, and the threshold was determined as the mean of the contrasts of the last five reversals. Each plotted threshold represents the mean of at least three measured thresholds. Different conditions were run in separate blocks. Results were obtained on three subjects (KTM, MAL, and MJS) with normal color vision as measured on the standard tests (Farnsworth–Munsell 100-Hue Test and The City University Colour Vision Test).

C. Digital Generation of Noise

Noise is a random fluctuation of luminance or chromaticity, $L(x)$, around the mean, L_0. Noise is characterized by a contrast function:

$$c(x) = [L(x) - L_0]/L_0 . \tag{2}$$

The variance σ^2 of the contrast function is called contrast power, defined as the integral of the square of the function. The square root of the power (standard deviation σ) is also known as the rms contrast C_{rms}. The Fourier transform of the autocorrelation of the contrast function is the power spectral density function $\rho(f)$ and represents the power at each spatial frequency.

To obtain the noise digitally we generated a discrete complex function in the Fourier domain (i.e., two arrays of N real numbers) whose values were drawn from Gaussian distributions. The resulting noise had a spectrum whose magnitude followed a Rayleigh distribution:

$$P(x) = (1/\sigma^2)x \exp[-x^2/(2\sigma^2)], \tag{3}$$

and its phase spectrum was uniformly distributed. The modulus of the complex array was then filtered with low-pass, high-pass, or symmetric notch filters, whose bandwidths were defined in octaves. To avoid ringing in the coordinate space, the edges of the filter were smoothed with a Hanning windown given by

$$W(f) = \cos^2[\pi(i - i_0)/(2k)], \tag{4}$$

where i_0 is the sample corresponding to the cutoff spatial frequency and k is the number of samples around the edge, which was four. Finally, we obtained the inverse fast Fourier transform of the filtered array, whose real part was an N-dimensional array that was added to the test stimulus. The imaginary part of the inverse Fourier transform was null, as we imposed the appropriate symmetry constraints in the Fourier domain.

The use of digital methods in the generation of the noise has particular consequences. The noise function in the Fourier domain is discretely defined by a number of samples whose spacing is Δf in a finite interval $[-f_N, f_N]$, where f_N is the Nyquist frequency of the system.[34,35] The exact values of the Nyquist frequency and the frequency sampling rate depend on the pixel size (Δx) and the array size (N). Because of these sampling limitations, real white noise (i.e., noise with all spatial frequencies) cannot be obtained. Noise generated digitally is bandpass with a lower frequency limit of Δf and an upper frequency limit of f_N. This noise, however, can be considered white for

the relevant visual mechanism if the Nyquist frequency is higher than the frequencies passed by the mechanism and the frequency sampling interval is smaller than the lowest frequency passed. For the same reasons, noise filtered with low-pass or high-pass filters is in fact bandpass. Below, we show results that demonstrate that the limits of our noise stimulus are far outside the passbands of the mechanisms detecting the 0.5-cycle/deg gratings, and for this reason we retain the terms low pass and high pass.

D. Power Spectrum Model with Use of $1/f$ Noise Power Density

To obtain the mechanism tuning functions it is necessary to postulate a model with several assumptions. We use a model similar to that in auditory psychophysics,[24] which has also been applied to visual masking.[19,36] The noise is represented by its power density function, $\rho(f)$, and the mechanism by its transfer function, $H(f)$. Thus the general masking equation is

$$P_t = P_0 + K \int_{-\infty}^{+\infty} \rho(f)|H(f)|^2 \mathrm{d}f\,, \tag{5}$$

where P_t, the power of the test at threshold, is proportional to c^2. P_0 is the power of the internal noise, which limits mechanism performance in the absence of external noise.[27,35] At power densities that are high compared with the internal noise, Eq. (5) indicates that test power at threshold is proportional (K) to the power of the noise transmitted by the filter (i.e., the filter's signal-to-noise ratio at threshold is constant).

One can solve Eq. (5) by choosing a masking stimulus whose power density simplifies the integral, such as low-pass, high-pass, bandpass, or notch noise. If noise power density is constant when noise bandwidth $\rho(f) = \rho_0$ is varied, Eq. (5) yields

$$P_t = P_0 + K\rho_0 \int_B |H(f)|^2 \mathrm{d}f\,, \tag{6}$$

where the limits of the integral are determined by B, representing the band of the noise filter in the frequency domain. Thus the total power of the noise band changes for different filter sizes.[19,36] The value of the integral is the square of the area of overlap between the filter and the transfer function of the mechanism (e.g., Fig. 1). On the basis of physiological and psychophysical data,[3,5,7–10,12,27–30] we have assumed that the visual mechanisms have equal-octave bandwidths. Consequently, in order to match the shapes of the visual mechanisms, we also defined the filters used for the noise on an octave scale. In Fig. 2 we illustrate two rectangular bandpass filters of 2 octaves each. One filter is centered at 2 cycles/deg and the other at 16 cycles/deg. In Figs. 2(a) and 2(c) the filters are represented on a linear spatial-frequency scale, and in Figs 2(b) and 2(d) the filters are shown on a log scale. The effects of the filters for white noise, $\rho(f) = \rho_0$, are shown in Figs. 2(a) and 2(b). The total power passed through the filters (shaded areas) is greater for the filter centered at 16 cycles/deg. For equal-octave bandwidths to pass equal power, the power density must vary as $1/f$, as illustrated in Figs. 2(c) and 2(d). A power density that varies as $1/f$ gives more power to the lower relative to the higher frequencies, thus compensating for the different spreads of the filters in linear coordinates [Fig. 2(c)]. Mathematical proof of this is given in Appendix A.

3. RESULTS

A. Thresholds Obtained in Broadband Noise

We performed control experiments with broadband noise to (1) assess the influence of the high spatial-frequency limit imposed by the use of the digitally generated noise for our experimental conditions, (2) estimate the influence of any luminance artifacts in the chromatic stimuli, and (3) test the assumption that the bandwidths of visual mechanisms are proportional to their peak spatial frequencies.

To assess whether the broadband noise is effectively white, we obtained thresholds with noise having an upper cutoff of 5.7, or 22 cycles/deg (the Nyquist frequency; see Appendix B). We obtained thresholds for luminance and chromatic gratings of 0.5 cycle/deg at a range of power densities, using broadband luminance and chromatic noise, respectively. The noise was filtered with a low-pass filter with an upper cutoff of 5.7 cycles/deg, providing a range of 3.5 octaves on either side of the test spatial frequencies. The open squares in Fig. 3(a) show thresholds for luminance stimuli for two subjects (MAL and MJS). The open squares in Fig. 3(b) show thresholds for chromatic stimuli (subjects MAL and KTM). At low

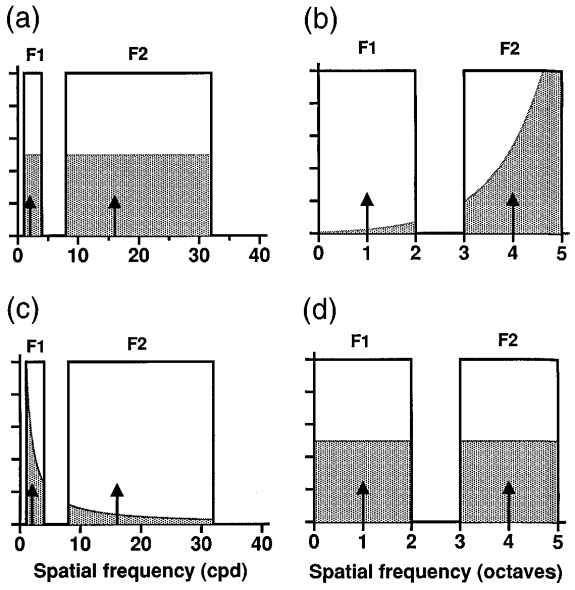

Fig. 2. Effect of constant and $1/f$-noise power densities. Two rectangular bandpass filters are shown, each of whose extent is 2 octaves, one centered at 2 cycles/deg and the other at 16 cycles/deg. Arrows mark central frequencies of the filters. (a), (b) Effects of a constant-noise power density ($\rho = \rho_0$); (c), (d) effects of a $1/f$-noise power density ($\rho = \rho_0/f$). In (a), (c) the filters are represented on a linear spatial-frequency scale, and the filter centered on the low frequency is narrower than the filter centered at a higher frequency. In (b) and (d) the filters are shown in octaves and thus have the same extent. The total power passed through the filters is represented by the shaded areas. For a constant-noise power density, the filter centered at 16 cycles/deg passes eight times more power than the filter centered at 2 cycles/deg. For a $1/f$-noise power density the power per octave is the same for the two bands. cpd, Cycles/deg.

power densities there is little masking, followed by a linear rise with a slope near 1. The effect of external noise in thresholds can be modeled by a system with an equivalent internal noise and limited sampling efficiency.[35,37,38] Thresholds were also obtained with noise whose spatial-frequency cutoff was the maximum frequency attainable with our apparatus ($f_N = 22$ cycles/deg, or +5.5 octaves) and are shown in the graphs by filled circles. There is no significant increase in masking for noise with higher frequencies. Thus both noises can be considered white for the mechanism at 0.5 cycle/deg. We kept the frequency content of chromatic noise below 5.7 cycles/deg to limit the possibility of artifacts resulting from chromatic aberration at high frequencies. The upper-frequency limit of luminance noise was also 5.7 cycles/deg.

We performed control experiments to assess the presence of putative luminance artifacts in the chromatic noise that may arise from residual chromatic aberrations or from an inaccurate isoluminant point. Thresholds for luminance test gratings were compared in the presence of chromatic noise and in luminance noise. We also measured thresholds for chromatic test gratings in luminance noise to estimate the effects of luminance artifacts on chromatic detection. The open circles in Fig. 3(a) show thresholds for luminance gratings in chromatic noise. Results show that luminance gratings are poorly masked by chromatic noise, which is in agreement with previous findings.[38] Figure 3(b) shows thresholds for chromatic gratings in luminance noise. These thresholds are lower than the unmasked threshold for both subjects except at the highest power densities. This small facilitatory effect is curious and resembles the facilitation of color detection in luminance contrast reported for sine-wave masking.[39,40]

Finally, we determined whether visual bandwidths are similar in linear coordinates or in octaves. We determined thresholds by using both constant and $1/f$ power densities for different test spatial frequencies. For a constant-noise power density, if the mechanism bandwidths are constant in octaves, the power passed by the high-frequency mechanisms will be greater than for the low-frequency mechanisms. Thus test thresholds will be expected to rise in proportion to test spatial frequency. If, however, the mechanisms have constant linear bandwidths, thresholds will remain constant. These effects are illustrated by Figs. 2(a) and 2(b) for mechanisms with rectangular transfer functions. For a $1/f$ power density the power is the same for all mechanisms if they have equal-octave bandwidths. In this case, constant thresholds at all frequencies would be predicted [Fig. 2(d)].

The thresholds for gratings of 0.5, 1, 1.4, 2, 2.8, and 4 cycles/deg were measured in broadband noise limited by 0.043 and 22.4 cycles/deg. The Gaussian envelope was varied so that there was a constant number of test cycles at all test frequencies. Figure 4(a) shows the thresholds for luminance gratings (subject MAL) and Fig. 4(b) for chromatic gratings (subject KTM). Threshold versus test frequency is shown by circles for noise whose power

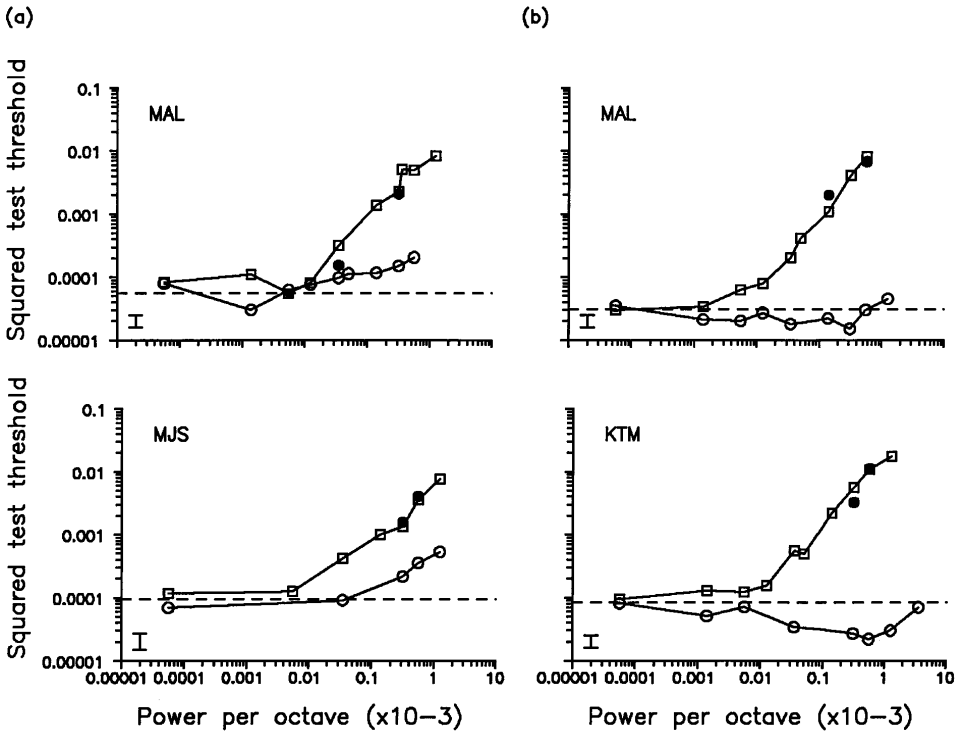

Fig. 3. Thresholds for luminance and chromatic test gratings of 0.5 cycle/deg in broadband luminance and chromatic noise. (a) Luminance contrast thresholds as a function of noise power density for subjects MAL and MJS, (b) isoluminant contrast thresholds for subjects MAL and KTM. Dashed lines, thresholds for the tests obtained in the absence of noise; open squares, thresholds (a) for the luminance test in luminance noise and (b) for the chromatic test in chromatic noise. The noise was filtered with a low-pass filter whose cutoff was 5.7 cycles/deg (+3.5 octaves above 0.5 cycle/deg). Filled circles, thresholds obtained with noise whose spatial-frequency cutoff was 22 cycles/deg (+5.5 octaves above 0.5 cycle/deg). Open circles, thresholds for (a) luminance gratings in the presence of chromatic noise (subjects MAL and MJS) and for (b) chromatic gratings in the presence of luminance noise (subjects MAL and KTM). An error bar in this and the following figures is shown at the bottom of each graph and represents twice the standard error of the mean.

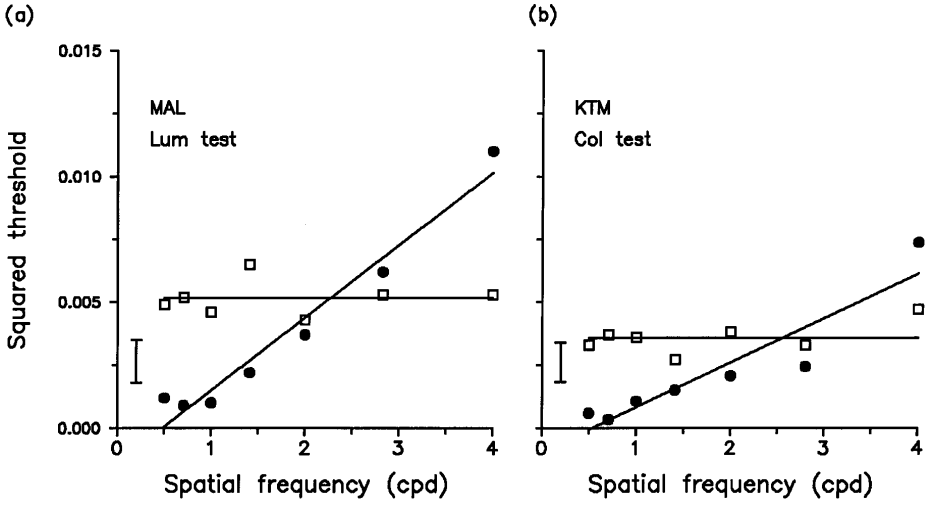

Fig. 4. Evidence for octave bandwidths. The thresholds for luminance and color test gratings of different spatial frequencies were measured in broadband noise of a constant power density of $\rho = 2.3 \times 10^{-4}$ (cycles/deg)$^{-1}$ (circles) and a $1/f$ power density of $\rho = 5.5 \times 10^{-4}$ octaves^{-1} (squares). (a) Squared thresholds for luminance gratings (subject MAL), (b) squared thresholds for chromatic gratings (subject KTM). Solid lines, linear regression of the data. cpd, Cycles/deg.

density was $\rho_0 = 2.3 \times 10^{-4}$ (cycles/deg)$^{-1}$. Using linear scales, the graphs show that thresholds in noise of constant power density rise linearly with spatial frequency. The thresholds for the same spatial frequencies were measured in broadband noise of power density $\rho = 5.5 \times 10^{-4}$ octaves^{-1} and are shown in the graphs as squares. These thresholds show no systematic variation with spatial frequency. These findings suggest that the bandwidths of visual mechanisms are proportional to their central spatial frequencies.

B. Thresholds Obtained in Low-Pass, High-Pass, and Symmetric Notched Noise

1. Bandwidths for Color and Luminance Mechanisms Centered at 0.5 Cycle/Deg

In this section we obtain thresholds in noise filtered with notches of different sizes at a given power density. We also use low-pass and high-pass noise of different cutoff frequencies at the same power density as the notched noise to estimate the lower and upper sides of the bandwidths. Figure 5 shows the thresholds for luminance (subjects MAL and MJS) and chromatic (subjects MAL and KTM) gratings (0.5 cycle/deg) in notched noise, with the notch size varying from 0.5 to 5 octaves. The power density was 5.5×10^{-4} octaves^{-1} ($\sigma = 0.1$) for the luminance noise and of 3.1×10^{-4} octaves^{-1} ($\sigma = 0.075$) for the chromatic noise. These values were chosen because they produced a tenfold elevation of luminance and color thresholds with broadband noise (subject MAL, Fig. 3). The abscissa shows notch width in octaves, and the ordinate shows the masked threshold. To obtain the bandwidths we assume that the shape of the mechanisms can be described by two exponential functions joined back to back:

$$\exp[+0.69(f - f_0)/B_l] \quad \text{if } f < f_0, \tag{7a}$$

$$\exp[-0.69(f - f_0)/B_u] \quad \text{if } f \geq f_0, \tag{7b}$$

where f is the spatial frequency in octaves of the test frequency, f_0 is the central frequency of the mechanism, and B_l and B_u are the lower and upper sides of the bandwidths (defined at half-height). The exponential shape has been used in auditory[24] and visual noise masking.[19,36] The central frequency of the most sensitive mechanism

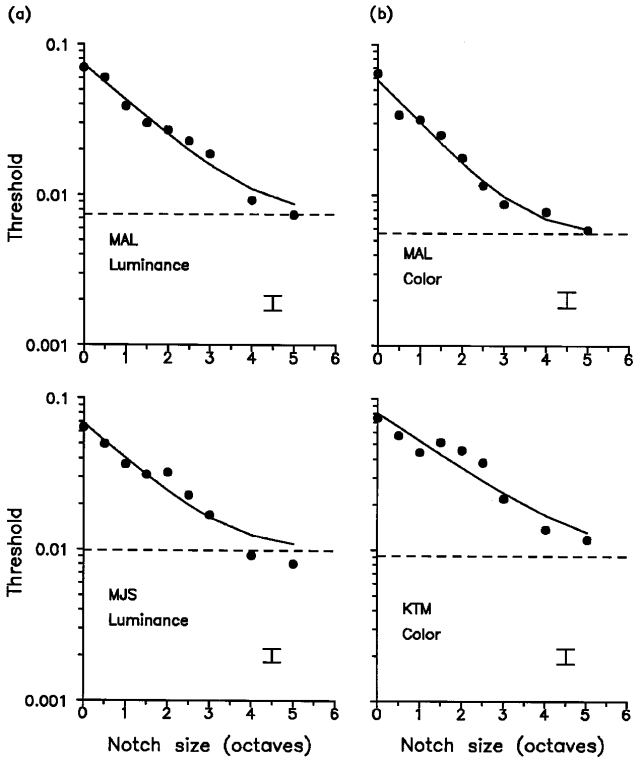

Fig. 5. Thresholds for luminance and chromatic gratings of 0.5 cycle/deg in notched noise. (a) Thresholds for luminance gratings for subjects MAL and MJS, (b) thresholds for chromatic gratings for subjects MAL and KTM. Power density was 5.5×10^{-4} octaves^{-1} ($\sigma = 0.1$) for luminance noise and 3.1×10^{-4} octaves^{-1} ($\sigma = 0.075$) for chromatic noise. Curves, model fitted to the data. The full bandwidths at half-height for luminance are 1.25 and 1.26 octave for subjects MAL and MJS, respectively, and for color they are 1.05 and 1.61 octave for MAL and KTM, respectively.

is assumed to be equal to the test spatial frequency ($f_0 = 0$). For symmetric notched noise we assume that the lower and upper sides of the mechanisms are equal: $B_l = B_u = B$. As we used a $1/f$ power density, the power of the test at threshold was given by Eq. (6) with f in octaves. The value of P_0 was fixed to the power of the test at threshold in the absence of external noise. We fitted the model to the data points for each set of results (solid curves) by varying the values of B and K. The value of the parameter K, which is the inverse of the sampling efficiency,[35,37,38] was close to 2 for all subjects and conditions. The estimates of full bandwidths at half-height for luminance contrast were 1.25 and 1.26 octaves for subjects MAL and MJS, respectively, and for color contrast the full bandwidths at half-height were 1.05 and 1.61 octaves for subjects MAL and KTM, respectively.

Figure 6 shows thresholds for the same luminance and color test gratings obtained in high-pass and low-pass noise (circles and squares, respectively). The power density of the low-pass and the high-pass noise was the same as for the notched noise for each subject and condition. The higher cutoff of the low-pass filter varied from −2.5 to +1.5 octaves of test frequency, and the lower cutoff of the high-pass filter varied from −1.5 to +2.5 octaves from 0.5 cycles/deg. The thresholds for high-pass noise with a cutoff of −1.5 octaves and low-pass noise with a cutoff of 1.5 octaves are equal to the thresholds obtained with the broadband noise (whose limits were −3.5 and +3.5 octaves), indicating that the lower and upper limits of the broadband noise do not influence the detection mechanism.

Figure 6 illustrates that the masking functions are asymmetric, with the lower side narrower than the upper side. This result was found previously with sine-wave and noise masking[3,12,36,41] and also with adaptation.[7,13] We obtained the values of K, B_l, and B_u that yielded the best fit to the thresholds obtained in low-pass and high-pass noise simultaneously. The model fit is shown in Fig. 6 by solid curves. The estimated lower and upper sides of the luminance mechanism were 0.39 and 0.84 octave, respectively, for subject MAL and 0.58 and 0.78 octave, respectively, for subject MJS. The differences between the lower and upper sides are significant within a 99% confidence interval. For the chromatic mecha-nism the lower and upper sides of the bandwidths were 0.45 and 0.55 octave, respectively, for subject MAL and 0.58 and 0.92 octave, respectively, for subject KTM. The differences between the lower and upper sides of the chromatic mechanism are significant only for subject KTM.

The full bandwidths were obtained by addition of the lower and upper sides of the tuning functions of the mechanisms, giving luminance full bandwidths of 1.22 and 1.36 for subjects MAL and MJS, respectively, and chromatic full bandwidths of 1.00 and 1.50 for subjects MAL and KTM, respectively. Bandwidths estimated with notched filters do not differ from the estimates obtained from low-pass and high-pass noise. Both estimates are equal within a confidence interval of 90%. If multiple mechanisms were intruding in test detection in the high- or low-pass noise, the bandwidths obtained would be narrower than for the notch-filtered noise. Thus these results indicate that off-frequency looking is negligible at these power densities. Off-frequency looking may, however, occur at higher power densities, and this is explored next.

2. Evidence for Off-Frequency Looking

We obtained test thresholds in high-pass, low-pass, and notched noise over a wide range of power densities. If more than one mechanism detects the test, or if the mechanism center shifts when the mask is low-pass or high-pass noise, the notched-noise thresholds will show an excess of masking.[19,21] We used low-pass and high-pass noise whose cutoff frequencies were 0.35 and 0.71 cycle/deg, respectively (±0.5 octave of 0.5 cycle/deg). The notched noise was the sum of the low-pass and high-pass noise bands, and thus the size of the notch was 1 octave. In Fig. 7, thresholds for luminance (subjects MAL and MJS) and chromatic (subjects MAL and KTM) gratings have been fitted by linear regression on a log−log scale. The thresholds in notch noise have a slope of 1 for all subjects and conditions, similar to those obtained with broadband noise (see Fig. 3). Thresholds in low-pass and high-pass noise, however, rise less steeply with noise power density than do the notched-noise thresholds. Previous research[12,15] indicates a relationship between the slope of threshold-versus-contrast functions and the intrusion of multiple mechanisms. Thus the reduced slope for low- and high-pass noise provides evidence of off-frequency looking.

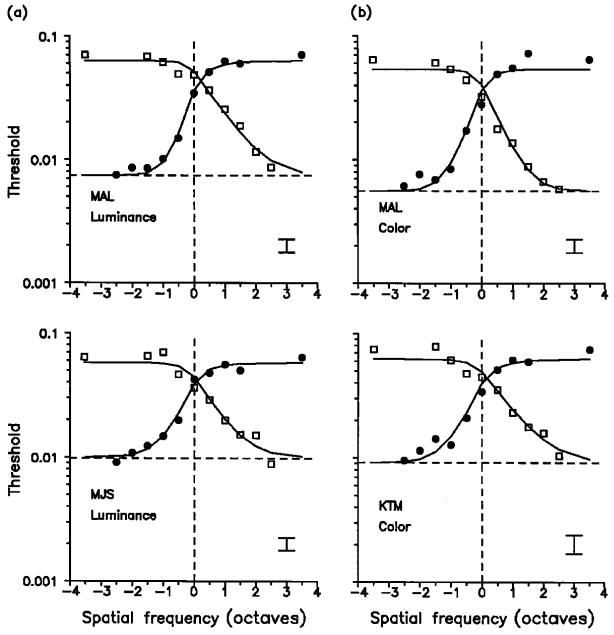

Fig. 6. Thresholds for luminance and color test gratings of 0.5 cycle/deg obtained in high-pass and low-pass noise. Thresholds (a) for luminance gratings for subjects MAL and MJS and (b) for chromatic gratings for subjects MAL and KTM. Circles, low-pass thresholds; squares, high-pass thresholds. The power density of the low-pass and high-pass noise was the same as for the notched noise for the corresponding subject and condition (see Fig. 5). Solid curves, model fit. For the luminance mechanism, $B_l = 0.39$ and $B_u = 0.84$ octave for MAL, and $B_l = 0.58$ and $B_u = 0.78$ octave for MJS. For the chromatic mechanism, $B_l = 0.45$ and $B_u = 0.55$ octave for MAL, and $B_l = 0.58$ and $B_u = 0.92$ for KTM. Thus the full bandwidths for luminance are 1.22 and 1.36 for MAL and MJS, respectively, and for color they are 1.00 and 1.50 for MAL and KTM, respectively.

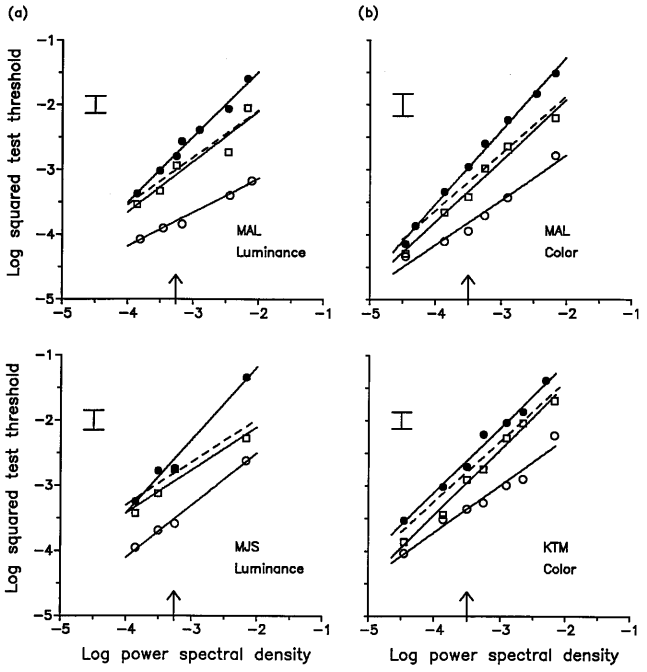

Fig. 7. Excess of masking. Thresholds (a) for luminance gratings for subjects MAL and MJS and (b) for chromatic gratings for subjects MAL and KTM. Open circles, low-pass noise (−0.5 octave); open squares, high-pass noise (+0.5 octave); filled circles, notched noise (1 octave). The low-pass and high-pass noise have cutoff frequencies of 0.35 and 0.71 cycle/deg, respectively (±0.5 octaves of 0.5 cycle/deg). Notch size, 1 octave. The data are fitted by a linear regression. Dashed lines, prediction for perfect summation of low-pass and high-pass thresholds obtained from the linear regressions. Arrows, value of the power density used in Figs. 5 and 6.

To estimate the degree of off-frequency looking, we plotted the prediction for perfect summation of low-pass and high-pass thresholds (obtained from the linear fits) as a dashed line. The thresholds for notched noise shown in Fig. 7 are greater than the linear summation prediction, especially at high power densities. The excess of masking at the highest power density (10^{-2} octaves^{-1}) for luminance gratings is 0.5 log unit for subject MAL and 0.8 log unit for subject MJS, and for chromatic gratings it is 0.5 log unit for subject MAL and 0.25 log unit for subject KTM. For all subjects there is no significant excess of masking at the lower power densities, and for KTM the excess of masking is significant only at the highest power density. We also note that there is no significant excess of masking at the power densities that we used to obtain the upper and lower sides of the bandwidths (marked with arrows, Fig. 7). At low powers the mechanism most sensitive to the test shows the highest signal-to-noise ratio, but, as noise power increases, mechanisms centered away from the noise band are likely to have a higher signal-to-noise ratio. This is probably the origin of the reduced slopes for low- and high-pass thresholds and thus of the variation in excess of masking with noise power.

Our results thus show evidence of off-frequency looking at high power densities for both color and luminance thresholds. There is also an absolute difference in the thresholds obtained with low-pass noise compared with the thresholds obtained with high-pass noise, which may reflect underlying asymmetries in the tuning functions.

3. *Control Experiments for the Noise Band and Gaussian Windowing*

In the threshold-versus-noise power functions of Fig. 7 it is clear that the low-pass noise is less effective than high-pass noise. This effect, which is particularly strong for luminance, may reflect genuine asymmetries in the visual mechanisms. On the other hand, the poor masking found for low-pass noise might be produced by the limitations of the generated noise. In particular, the lower limit for the spatial frequencies contained in the noise was 0.043 cycle/deg. Thus nominally low-pass noise with a cutoff of 0.25 cycle/deg (−1 octave of 0.5 cycle/deg) is in fact bandpass with a bandwidth of 2.5 octaves. Another possible origin of the low thresholds obtained in low-pass noise is the effect of the spatial Gaussian windowing on the noise. The window redistributes the noise mask power, and this may reduce mask efficiency at the low frequencies. Neither of these effects affects previous conclusions about off-frequency looking, as the low-pass noise is identical when presented alone or as part of the notched noise. In order to assess these effects, however, we performed two control experiments with low-pass noise.

We first assessed the importance of the passband for the nominally low-pass noise. We obtained thresholds for two luminance gratings (0.5 and 2 cycles/deg) in digitally generated low-pass noise with −1 octave cutoff. Thus the upper cutoff for the 0.5-cycle/deg test was 0.25 cycle/deg and was 1 cycle/deg for the 2-cycle/deg test. Taking into account the low-frequency limit, the two noise bands have bandpass characteristics with bandwidths of 2.5 and 4.5 octaves. Assuming that the detection mechanisms for the two test stimuli are similar, the effect of the noise on the test thresholds should be equivalent if there is no influence of the low-frequency limit. On the other hand, if more masking is found with the effectively wider band for the 2-cycle/deg test, we would conclude that the lower limit of the digital noise is within the bounds of the mechanism detecting 0.5 cycle/deg. The size of the Gaussian envelope was set to a constant number of test cycles for the 0.25- and 2-cycle/deg tests. The results are shown in Fig. 8(a) for subject MAL at a range of power densities. Horizontal lines show the unmasked thresholds for the two test stimuli. The threshold elevations for 2 and 0.5 cycles/deg are similar even though the size of the noise band was wider for the 2-cycle/deg test. The threshold elevations for the 0.5-cycle/deg test in low-pass noise with a cutoff of 1 cycle/deg (+1 octave) are also shown in the figure (filled symbols) to demonstrate that this noise band is an effective mask. The same noise band produces a tenfold elevation for the 0.5-cycle/deg test but only a twofold elevation for the 2-cycle/deg test at a power density of 5.5×10^{-4} octave^{-1}.

We also examined the influence of the spatial extent of the mask. The thresholds for 2 cycle/deg in low-pass noise with a 1-cycle/deg cutoff were measured with a Gaussian envelope for test and mask of four times greater width (12 test cycles). The thresholds for this new condition [Fig. 8(b)] were reduced somewhat (1.7 times) compared with the data given above (a Gaussian width of three test cycles). More importantly, however, there are no significant differences in the threshold elevations with noise. This indicates that the Gaussian windowing does

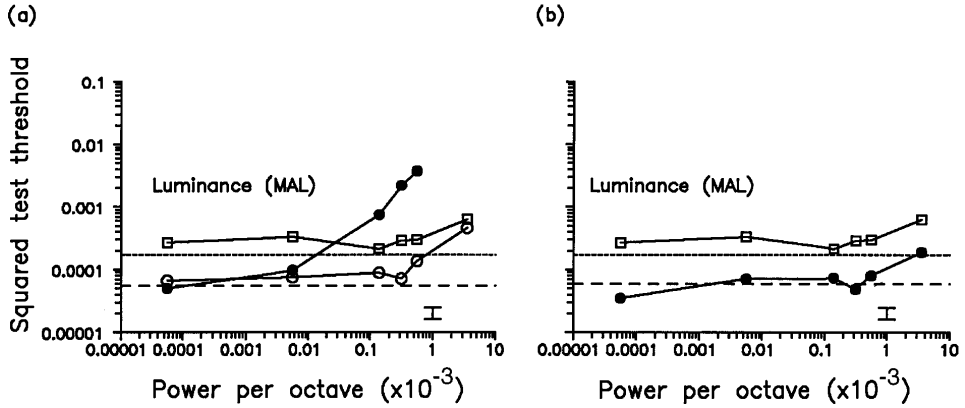

Fig. 8. Results for subject MAL. (a) Effect of the lower spatial-frequency limit of the noise. Thresholds for luminance test gratings of 0.5 cycle/deg (open circles) and 2 cycle/deg (open squares) in low-pass noise with −1 octave cutoff. For the 0.5-cycle/deg test the effective noise band was 2.5 octaves, and for the 2-cycle/deg test it was 4.5 octaves (see text). The Gaussian envelope was a constant number of test cycles. Horizontal lines, unmasked thresholds for the two test stimuli. Filled circles, thresholds for the 0.5-cycle/deg test in low-pass noise of 1-cycle/deg cutoff (+1 octave). (b) Effect of Gaussian windowing on the noise mask. Circles, thresholds for a 2-cycle/deg luminance grating in low-pass noise (1-cycle/deg upper cutoff) when the stimulus (test and mask) width was 12 test cycles. The data obtained for a frequency of 2 cycle/deg with a Gaussian width of three test cycles have been replotted in the figure for comparison (squares). The increased number of cycles reduced threshold by a factor of 1.7. The figure shows that there are no significant differences in threshold elevation produced by the noise.

not reduce mask effectiveness,[42] and we conclude that the asymmetries for noise masking reflect a genuine asymmetric tuning of the detection mechanisms.

4. DISCUSSION

Noise masking has several advantages over the technique of sinusoidal masking. The combination of sinusoidal gratings of different spatial frequencies produces local changes in the stimulus that subjects are able to detect.[43–48] In noise masking the variability of noise removes any local cues, and the appearance of the stimulus remains more uniform through changes in mask contrast and frequency. In addition, sinusoidal masks produce subthreshold facilitation,[49–52] which may distort the estimates of bandwidth.[12,53,54] One problem that the use of noise masking does not necessarily eliminate is the presence of off-frequency looking. Comparing thresholds obtained in notched noise with thresholds in low-pass and high-pass noise, we found a significant excess of masking at the highest-noise power densities for both luminance and chromatic stimuli. This indicates an intrusion of multiple mechanisms in test detection in the low-pass and high-pass noise.

There is also evidence that off-frequency looking biases the estimates of the tuning properties of other visual mechanisms. For example, bandwidths of the channels that are selective for the spatial frequency of binocular disparity estimated from notched-noise thresholds were more than twice as broad as estimates from narrow-band thresholds.[22] In a study of orientation selectivity in cats and humans, Blake and Holopigian[20] used noise of two orientations symmetrically placed about the test orientation to discourage the observers from employing an off-channel strategy. They found narrower bandwidths compared with those measured with only one orientation of noise. We do not find any narrowing in our estimates of the bandwidths obtained with low- and high-pass noise, because low power densities were used, for which off-frequency looking was negligible. A narrowing of the low- and high-pass bandwidths would be expected if higher powers were used.

The averaged (over two subjects) full bandwidths that we obtain with notch noise is 1.3 octaves for both the luminance and the chromatic mechanisms. Previous studies of the tuning properties of the luminance mechanisms with use of noise masking give similar bandwidth estimates. Luminance full-bandwidth estimates obtained from narrow-band, high-pass, and low-pass noise of approximately 2 octaves were reported by Stromeyer and Julesz.[5] Their results agree with those of Henning *et al.*,[36] who estimated the bandwidths by using a similar method. Pelli[19] reported a 1.6-octave exponential channel centered at 4 cycle/deg from thresholds in low- and high-pass noise and a somewhat narrower one from thresholds in narrow-band noise. To our knowledge, there are no previous studies on the spatial tuning of chromatic mechanisms with noise.

Although notched noise prevents off-frequency looking and yields estimates of the passbands that are closer to those of the underlying mechanisms, it has the disadvantage that all information about asymmetries is lost. The lower and upper sides of the mechanisms, however, can be estimated from low-pass and high-pass thresholds. At low power densities off-frequency looking in low-pass and high-pass noise is negligible, and our estimates of the lower and upper sides of the bandwidths of the chromatic and luminance mechanisms should be reliable. The asymmetry of the tuning functions is significant for two subjects for luminance detection and for one subject for color detection.

These asymmetries are not caused by limitations in the noise stimuli themselves. Such asymmetries have appeared before in masking and adaptation studies for color and luminance gratings, but their explanation remains unclear.[3,7,12,13,36,41] We previously suggested that their origin could be the intrusion of multiple mechanisms in the detection of the test[12]; however, since we now find that these asymmetries remain in the absence of off-frequency looking, we conclude that they are inher-

ent to the detection mechanism. At high power densities, however, the intrusion of multiple mechanisms may still potentially produce additional asymmetries of the tuning functions. This effect is reflected in the difference of the slopes for the low-pass and high-pass thresholds in some of the graphs of Fig. 7. Asymmetric notched-noise masking could be used[23,24] for estimating the interaction between the mechanism asymmetries and the degree of off-frequency looking.

Previously we estimated the bandwidths of the color and luminance mechanisms at different spatial frequencies, using simultaneous sine-wave masking.[12] We obtained bandwidth estimates by fitting Gaussian functions in octaves to the threshold elevations. For 0.5 cycle/deg and using the combined data of the same three subjects, we reported average bandwidths of 2.4 and 2.0 octaves for the chromatic and the luminance mechanisms, respectively, differing from the bandwidths that we find here (1.3 for both color and luminance). To make a fair comparison between our two estimates of bandwidth, we refitted the sine-wave masking data, using the asymmetric exponential functions given by Eqs. (7a) and (7b) instead of the symmetric Gaussians that we used previously. The average over the three subjects of the bandwidth estimates for the mechanism centered at 0.5 cycle/deg now becomes 1.43 octaves for luminance and 1.05 for color. These values are close to those that we obtain with the noise masking. However, only 5 or 6 data points per subject were available for the fits to the sine-wave masking data, whereas 9 data points were used for notched noise and 20 data points for the combined low- and high-pass noise data. Thus, aside from the methodological improvements of noise masking discussed above, the bandwidth estimates from the noise-masking data will be more accurate. Furthermore, the similarity of the data obtained from the present study and the previous studies suggest that off-frequency looking was not a significant contaminant of the sine-wave masking data.

In conclusion, these results reveal that color and luminance contrast are processed by similar bandpass mechanisms of 1.3 octaves and that the mechanisms are asymmetric, with a steeper lower side. There is evidence that both color and luminance mechanisms have bandwidths that are proportional to their center frequencies (constant in octaves). These results support the general conclusion that color vision, like luminance vision, uses bandpass filtering in the encoding of the visual image.

APPENDIX A

Assuming that the bandwidths of the mechanisms are similar in octaves, their transfer functions $H(\,)$ are better represented as a function of $\log(f)$. Substituting all terms in Eq. (5) according to the change of variable $[f \rightarrow y = \log(f)]$ for a power density $\rho(f) = \rho_0$, results in

$$P_t = P_0 + K\rho_0 \int_B |H(y)|^2 \exp(y)\mathrm{d}y\,. \tag{A1}$$

Comparing Eqs. (5) and (A1), one can see that the effective noise power density in Eq. (A1) is $\rho(y) = \rho_0 \exp(y)$ or $\rho(f) = \rho_0 f$, which varies proportionally with spatial frequency. If we take instead a $1/f$ power density, $\rho(f) = \rho_0/f = \rho_0 \exp(-y)$, Eq. (5) yields

$$P_t = P_0 + K\rho_0 \int_B |H(y)|^2 \mathrm{d}y\,, \tag{A2}$$

which is formally equivalent to Eq. (6). Thus the use of a power density constant in octaves $[\rho(f) = \rho_0/f]$ according to Eq. (5) produces an equivalent effect on octave bands as constant power density $[\rho(f) = \rho_0]$ on linear bands.

APPENDIX B

The absolute value of power density depends on the limitations imposed by the geometry of the display. In our case the pixel size was $\Delta x = 0.036$ cm where the distance of the subject to the display was $D = 90$ cm. The number of pixels available was $N = 1024$. With these values the sampling rate in frequency was $\Delta f = 0.043$ cycle/deg and the Nyquist frequency was $f_N = 22$ cycles/deg, which spans approximately a band of 9 octaves of 0.5 cycle/deg. Thus the power density constant in linear coordinates is given by

$$\rho^{\mathrm{lin}}(f) = {C^2}_{\mathrm{rms}}/2f_N = 0.023{C^2}_{\mathrm{rms}} \tag{B1}$$

in $(\mathrm{cycles/deg})^{-1}$, and power density constant in octaves is given by

$$\rho^{\log}(\log f) = {C^2}_{\mathrm{rms}}/2\log_2(f_N/\Delta f) = 0.055{C^2}_{\mathrm{rms}} \tag{B2}$$

in $\mathrm{octaves}^{-1}$, where $\log_2(\,)$ is the logarithm in base 2. ${C_{\mathrm{rms}}}^2$ for a Rayleigh distribution is $2\sigma^2$. Notice that the band is defined as including the negative as well as the positive frequencies.

ACKNOWLEDGMENTS

We thank Robert Hess for his help during the development of this work. We thank Eric Fredericksen and William McIlhagga for their useful comments on the first draft of the manuscript. We thank Marcel Sankeralli for acting as a subject. This research was supported by grant 10819 to K. T. Mullen from the Medical Research Council of Canada.

REFERENCES

1. F. W. Campbell and J. G. Robson, "Application of Fourier analysis to the visibility of gratings," J. Physiol. **197,** 551–556 (1968).
2. N. Graham and J. Nachmias, "Detection of patterns containing two spatial frequencies: a test of single and multichannel models," Vision Res. **11,** 251–259 (1971).
3. G. E. Legge and J. M. Foley, "Contrast masking in human vision," J. Opt. Soc. Am. **70,** 1458–1471 (1980).
4. B. E. Carter and G. B. Henning, "The detection of gratings in narrow-band visual noise," J. Physiol. **219,** 355–365 (1971).
5. C. F. Stromeyer III and B. Julesz, "Spatial-frequency masking in vision: critical bands and spread of masking," J. Opt. Soc. Am. **62,** 1221–1232 (1972).
6. M. B. Sachs, J. Nachmias, and J. C. Robson, "Spatial-frequency channels in human vision," J. Opt. Soc. Am. **61,** 1176–1186 (1971).
7. C. Blakemore and F. W. Campbell, "On the existence of neurons in the human visual system selectively sensitive to the orientation and size of retinal images," J. Physiol. **203,** 237–260 (1969).

8. K. K. De Valois and E. Switkes, "Simultaneous masking interactions between chromatic and luminance gratings," J. Opt. Soc. Am. **73,** 11–18 (1983).
9. E. Switkes, A. Bradley, and K. K. De Valois, "Contrast dependence and mechanisms of masking interactions among chromatic and luminance gratings," J. Opt. Soc. Am. A **5,** 1149–1162 (1988).
10. R. A. Humanski and H. R. Wilson, "Spatial frequency mechanisms with short-wavelength-sensitive cone inputs," Vision Res. **32,** 549–560 (1992).
11. R. Pandey and R. L. P. Vimal, "Threshold elevation curves for the red–green channel estimated by oblique masking," Invest. Ophthalmol. Vis. Sci. Suppl. **34,** 751 (1993).
12. M. A. Losada and K. T. Mullen, "The spatial tuning of chromatic mechanisms identified by simultaneous masking," Vision Res. **34,** 331–341 (1994).
13. A. Bradley, E. Switkes, and K. K. De Valois, "Orientation and spatial frequency selectivity of adaptation to color and luminance gratings," Vision Res. **28,** 841–856 (1988).
14. H. R. Wilson, D. K. McFarlane, and G. C. Phillips, "Spatial frequency tuning of orientation selective units estimated by oblique masking," Vision Res. **23,** 873–882 (1983).
15. J. M. Foley and Y. Yang, "Forward pattern masking: effects of spatial frequency and contrast," J. Opt. Soc. Am. A **8,** 2026–2037 (1991).
16. J. M. Foley and G. M. Boynton, "Simultaneous pattern masking: mechanisms are revealed by threshold versus masker contrast functions and the direct measurement of masking sensitivity," Invest. Ophthalmol. Vis. Sci. Suppl. **33,** 1256 (1992).
17. C. W. Tyler, L. Barghout, and L. L. Kontsevitch, "Surprises in analyzing the mechanisms underlying threshold elevation functions," Invest. Ophthalmol. Vis. Sci. Suppl. **34,** 819 (1993).
18. R. D. Patterson, "Auditory filter shapes derived with noise stimuli," J. Acoust. Soc. Am. **59,** 640–654 (1976).
19. D. G. Pelli, "Channel properties revealed by noise masking," Invest. Ophthalmol. Vis. Sci. Suppl. **19,** 44A (1980).
20. R. Blake and K. Holopigian, "Orientation selectivity in cats and humans assessed by masking," Vision Res. **25,** 1459–1467 (1985).
21. M. E. Perkins and M. S. Landy, "Nonadditivity of masking by narrow-band noises," Vision Res. **31,** 1053–1065 (1991).
22. A. B. Cobo-Lewis and Yei-Yu Yeh, "Selectivity for the spatial frequency of binocular disparity modulation," Invest. Ophthalmol. Vis. Sci. Suppl. **34,** 1439 (1993).
23. R. D. Patterson and I. Nimmo-Smith, "Off-frequency listening and the auditory filter asymmetry," J. Acoust. Soc. Am. **67,** 229–241 (1980).
24. R. D. Patterson and B. C. J. Moore, "Auditory filters and excitation patterns as representations of frequency resolution," in *Frequency Selectivity in Hearing*, B. C. J. Moore, ed. (Academic, London, 1986), pp. 123–177.
25. R. F. Hess and R. J. Snowden, "Temporal properties of human visual filters: number, shapes, and spatial covariation," Vision Res. **32,** 47–59 (1992).
26. K. T. Mullen, "The contrast sensitivity of human color vision to red–green and blue–yellow chromatic gratings," J. Physiol. **359,** 381–409 (1985).
27. R. L. De Valois, D. G. Albrecht, and L. G. Thorel, "Spatial frequency selectivity of cells in macaque visual cortex," Vision Res. **22,** 545–559 (1982).
28. D. J. Tolhurst and I. D. Thompson, "On the variety of spatial frequency selectivities shown by neurons in area 17 of the cat," Proc. R. Soc. London Ser. B **213,** 183–199 (1982).
29. D. J. Field and D. J. Tolhurst, "The structure and symmetry of simple-cell receptive field profiles in the cat's visual cortex," Proc. R. Soc. London Ser. B **228,** 279–400 (1986).
30. D. J. Field, "Scale-invariance and self-similar 'wavelet' transforms: an analysis of natural scenes and mammalian visual systems," in *Wavelets, Fractals and Fourier Transforms*, M. Farge, J. C. R. Hunt, and J. C. Vassilicos, eds. (Clarendon, Oxford, 1993), pp. 151–193.
31. K. T. Mullen and J. C. Boulton, "Absence of smooth motion perception in color vision," Vision Res. **32,** 483–488 (1992).
32. J. D. Moreland, "Spectral sensitivity measured by motion photometry," Documenta Ophthalmol. Proc. Ser. **33,** 61–66 (1982).
33. P. Cavanagh, "Reconstructing the third dimension: interactions between color, texture, motion, binocular disparity and shape," Comput. Vision Graphics Image Process. **37,** 171–195 (1987).
34. A. Burgess, "Effect of quantization noise on visual signal detection in noisy images," J. Opt. Soc. Am. A **2,** 1421–1428 (1985).
35. G. E. Legge, D. Kersten, and A. E. Burgess, "Contrast discrimination in noise," J. Opt. Soc. Am. A **4,** 391–404 (1987).
36. G. B. Henning, B. G. Hertz, and J. L. Hinton, "Effects of different hypothetical detection mechanisms on the shape of spatial frequency filters inferred from masking experiments: I. Noise masks," J. Opt. Soc. Am. **71,** 574–581 (1981).
37. D. G. Pelli, "The quantum efficiency of vision," in *Vision, Coding and Efficiency*, C. B. Blakemore, ed. (Cambridge U. Press, Cambridge, 1990), pp. 3–24.
38. K. R. Gegenfurtner and D. C. Kiper, "Contrast detection in luminance and chromatic noise," J. Opt. Soc. Am. **9,** 1880–1888 (1992).
39. K. T. Mullen and M. A. Losada, "Evidence for separate pathways for color and luminance detection mechanisms," J. Opt. Soc. Am. A **11,** 3136–3151 (1994).
40. G. R. Cole, C. F. Stromeyer III, and R. E. Kronauer, "Visual interactions with luminance and chromatic stimuli," J. Opt. Soc. Am. A **7,** 128–140 (1990).
41. C. F. Stromeyer III and S. Klein, "Spatial frequency channels in human vision as asymmetric (edge) mechanisms," Vision Res. **14,** 1409–1420 (1974).
42. D. Kersten, "Spatial summation in visual noise," Vision Res. **24,** 1977–1990 (1984).
43. G. B. Henning, B. G. Hertz, and D. E. Broadbent, "Some experiments bearing on the hypothesis that the visual system analyses spatial patterns in independent bands of spatial frequency," Vision Res. **15,** 887–897 (1975).
44. R. F. Quick, W. W. Mullins, and T. A. Reichert, "Spatial summation effects on two-component grating thresholds," J. Opt. Soc. Am. **68,** 116–121 (1978).
45. J. H. T. Jamar and J. J. Koenderink, "Contrast detection and detection of contrast modulation for noise gratings," Vision Res. **4,** 511–521 (1985).
46. D. R. Badcock and A. M. Derrington, "Detecting the displacement of spatial beats: no role for distortion products," Vision Res. **29,** 731–739 (1989).
47. J. P. Thomas, "Effect of static-noise and grating masks on detection and identification of grating targets," J. Opt. Soc. Am. A **2,** 1586–1592 (1985).
48. J. Nachmias, "Masked detection of gratings: the standard model revisited," Vision Res. **33,** 1359–1365 (1993).
49. J. Nachmias and R. V. Sansbury, "Grating contrast: discrimination may be better than detection," Vision Res. **14,** 1039–1042 (1974).
50. C. F. Stromeyer III, S. Klein, B. M. Dawson, and L. Spilmann, "Low spatial-frequency channels in human vision: adaptation and masking," Vision Res. **22,** 225–233 (1982).
51. J. M. Foley and G. E. Legge, "Contrast detection and near-threshold discrimination in human vision," Vision Res. **21,** 1041–1053 (1981).
52. D. G. Pelli, "Uncertainty explains many aspects of visual contrast detection and discrimination," J. Opt. Soc. Am. A **2,** 1508–1531 (1985).
53. J. M. Foley, "Pattern masking phenomena require a new model of human pattern vision mechanisms," Invest. Ophthalmol. Vis. Sci. Suppl. **34,** 819 (1993).
54. H. D. Speed and J. Ross, "Spatial frequency tuning of facilitation by masks," Vision Res. **32,** 1143–1148 (1992).